ISSN 1052-6188, Journal of Machinery Manufacture and Reliability, 2024, Vol. 53, No. 5, pp. 432–442. © Pleiades Publishing, Ltd., 2024.

RELIABILITY, STRENGTH, AND WEAR RESISTANCE OF MACHINES AND STRUCTURES

Tribological and Thermodynamic Properties of the High Entropy Alloys CrMnFeCoNi and CuCrMnFeCoNi, Their Stability, and Structure Prediction

V. I. Kolesnikov[a], A. A. Guda[a], I. V. Kolesnikov[a], S. A. Guda[a], K. N. Polityko[a,*], and Yu. A. Abzaev[b]

[a] *Rostov State Transport University, Rostov-on-Don, Russia*

[b] *Tomsk State University of Architecture and Civil Engineering, Tomsk, Russia*

**e-mail: politykokirill@yandex.ru*

Received April 16, 2024; revised June 13, 2024; accepted June 15, 2024

Abstract—High-entropy coatings based on 3D metals have a unique combination of strength and ductility over a wide temperature range and can be obtained using vacuum ion-plasma magnetron sputtering technology. However, the model calculations of the thermomechanical properties of such alloys are complicated by a lack of stable and equilibrium lattices with complete structural information. This article implements prediction of the stability of the phases of an equiatomic high-entropy coating of CrMnFeCoNi by the inverse convex hull method. The thermodynamic and mechanical properties were determined. It was found that, up to room temperature, the medium-entropy, 4-element alloy of composition MnFeCoNi also belongs to the stable phases.

Keywords: CrMnFeCoNi, MnFeCoNi, high-entropy alloys, mechanical, tribological, thermodynamic properties, stability of high-entropy alloys

DOI: 10.1134/S1052618824700985

The use of functional coatings in heavily loaded tribosystems in aviation, transport, and mechanical engineering is characterized by increased attention to the problems of friction and wear. The relevance of this is due to the safety and reliability of friction units, as well as the desire to save expensive materials for friction units in which the working area is the tribological interface. These problems can be solved by applying vacuum ion-plasma wear-resistant coatings to contact surfaces. High-entropy alloys (HEAs), a hitherto insufficiently studied class of materials, were chosen as the object of research. Research efforts have been aimed not only at studying the physical, mechanical, and tribological characteristics of HEAs, but also at determining their stability over a wide temperature range. The role of temperature in the mechanism of friction and wear is decisive and characterizes the strength and deformation properties of materials.

High-entropy materials with an equiatomic content of components are characterized by high configurational entropy, low atomic diffusion, lattice distortions, and the formation of simple cubic lattices (fcc. OCC, GPU) [1–9]. In [1], it was first shown that CoCrFeMnNi is single-phase and is characterized by noticeable microstructural stability over a long period of time. It was found that, under tension, the yield strength, ultimate strength, and elongation to failure simultaneously increase as the temperature decreases from room temperature to 77 K. High fracture toughness has been established [2]. The peculiarities of the mechanical properties of CoCrFeMnNi are usually associated with the peculiarities of the elastic characteristics of the alloy and the slow kinetics of diffusion at elevated temperatures. Interest in HEAs is also associated with exceptional strength characteristics at high temperatures, ductility, and impact strength at cryogenic temperatures [7]. Due to the lack of a crystallographic base of HEAs in the literature, the study of the structural state of HEAs by the Rietveld method [10, 11], as well as the model thermodynamic and mechanical properties of HEAs of various elemental compositions, is significantly complicated. There is no information in the literature about the HEA CoCrFeMnNi with complete crystallographic information: space group, atomic coordinates, lattice parameters, site occupancy, etc. As a consequence, it is impossible to study the thermodynamic and mechanical properties of such materials. It seems relevant to identify the HEA structures of CrMnFeCoNi, and on their basis conduct study of the thermodynamic and

mechanical properties at finite temperatures. Prediction of equilibrium, stable single-phase alloy lattices of CrMnFeCoNi can be realized by the inverse convex hull method [12] (InverseHubWeb) in the temperature range $T = 300 - T_{melt}$ K, evolutionary code USPEX [13, 14] with the VASP interface, equilibrium states in the vaspkit code [15]. Subsequent ab initio calculations of the structural and thermodynamic characteristics of the lattices in the Phonopy code [16] and Vasp on the Blochi supercomputer.

This article is a prediction of the structural and equilibrium state and stability of the HEA CrMnFeCoNi with a simple cubic (SC) lattice with analysis of the energy, the entropy of mixing of binary alloys near the melting point in the framework of the Miedema model, and the entropy of mixing of the 5-element composition CrMnFeCoNi. We forecast stable phases of CrMnFeCoNi by the evolutionary method, and the temperature stability ranges by the InveseHubWeb code in the temperature range $T = 300 - T_{melt}$ K. We study the thermodynamic and mechanical properties of the HEA CrMnFeCoNi with an SC grid in a wide temperature range, as well as the physical, mechanical, and tribological properties of the CuCrMnFeCoNi coating.

MATERIALS AND METHODS

The emergence of a new class of materials, high-entropy alloys (HEAs), is explained by the fact that, if a multicomponent system is formed in the form of a single-phase substitutional solid solution, then its configurational entropy component will be an order of magnitude higher than the other components. In this case, the Gibbs energy of such a system becomes minimal and gives the system high thermodynamic stability. Moreover, the greater the number of components n mixed in the solution, the higher the stability of the system (the minimum set is considered $n = 4–5$). In this case, an alloy can be considered high-entropy if it satisfies the following criteria: the difference in atomic sizes (the atomic radii of components δ must be within $0\% \le \delta \le 8.5\%$); the enthalpy of mixing ΔH_{mix} must be within 7 kJ/mol$\le \Delta H_{mix} \le$ 22 kJ/mol; and the entropy of mixing ΔS_{mix} should be within 11 J/(K mol) $\le \Delta S_{mix} \le$ 19.5 J/(K mol). ΔS_{mix} determined by Boltzmann is $\Delta S_{mix} = -R\sum_{i=1}^{n} c_i \ln c_i$, at an equiatomic concentration of components $C_i = 1/n$ and $\Delta S_{mix} = R\ln(n)$, where $R = 8.314$ J/(K mol) is the universal gas constant. With an increasing number of components n, the equiatomic composition entropy of mixing ΔS_{mix} grows: so with $n = 5$, $\Delta S_{mix} =$ 13.8 J/(K mol); at $n = 10$, $\Delta S_{mix} = 19$ J/(K mol).

To enhance the tribological emphasis of the coating, copper was introduced into the composition of CrMnFeCoNi powder targets: CuCrMnFeCoNi. Thus, the composition of the real targets from which coatings were deposited onto the samples corresponded to the equiatomic concentration of the components of the CuCrMnFeCoNi system. At the same time, increasing the number of components to six increases the entropy of mixing to the value $\Delta S_{mix} = 15$ J/(K mol) and the system under study becomes even more high-entropy.

Coatings of the CuCrMnFeCoNi system were applied in the magnetron sputtering mode using a BRV600 vacuum unit (manufactured by BelRosVak LLC, Minsk, Belarus) equipped with a powerful ion source. The coating was applied for samples made of structural steel 40KhN2MA. The physical and mechanical characteristics of 40KhN2MA steel after quenching and low tempering with a martensitic structure make up $H = 5.2$ GPa; $E = 200$ GPa; $H/E = 0.026$ is resistance to elastic deformation; and $H^3/E^2 = 0.00352$ GPa is resistance to plastic deformation.

The magnetron used targets made by powder metallurgy. Samples made of 40KhN2MA steel, made in the form of a plate with dimensions 50 × 30 × 5 mm, were subjected to ion etching with Ar+ at a chamber pressure of ~0.7 Pa and a temperature of ~400°C before the coating stage and a mixing voltage of 1000 V for five minutes.

To study physical and mechanical samples at the nano- and microscale level, the NanoTest 600 measuring platform was used. The elastic modulus was determined using the continuous indentation method [17] E and hardness H, and H/E and H^3/E^2. When measuring in the micro range (load less than $2H$ and indentation depth more than 0.2 μm), a tetrahedral Vickers indenter was used; for work in the nanorange (indentation depth no more than 0.2 μm), a triangular Berkovich indenter was used. Test conditions and processing of the obtained data were carried out in accordance with GOST 8.748-2011 [18].

Tribological tests of coatings were carried out on a TRB friction machine using the “pin scheme–plate” either with reciprocating movement of the plate (coated sample) with a frequency of 10 Hz and an amplitude of 800 μm, or with radial movement along a circle with a diameter of 6 mm. The normal force on the pin varied discretely and amounted to 1.5 and 10 N. The counter sample was a ball with a diameter of 6.35 mm fixed in a pin made of Cermet (hard alloy) WC–Co. Due to the fact that the ball is stationary

in the pin, the tests are classified as sliding friction. The test duration was 50000 cycles. We determined such tribological parameters as the friction coefficient μ, the intensity of volumetric wear of the sample J and counterbodies JK, and the length of the path (friction path) L traversed by the sample before the coating is destroyed and measured in meters.

Studying the stability of a CrMnFeCoNi alloy of equiatomic composition can be carried out using the InverseHubWeb method [12]. InverseHubWeb carries out ab initio calculations of the free energy of structures based on the cluster method [12]. The stability of phases of known equiatomic composition is determined based on calculations of the energy of formation and mixing in the convex hulls of single HEAs based on Material Project standards. Details of the estimates are discussed in [12]. In the InverseHubWeb method, the results are presented on a flat 2D diagram with the energy of formation and mixing axes (Fig. 1), the level of the latter is determined by the driving force of the phase separation of the HEA into low-component reactants. Alloys with mixing energy exceeding the zero level are classified as quasi-stable structures. The vertices of multidimensional convex hulls are stable phases (convex hull reactants) or intermetallic alloys from the Material Project crystallographic database. The composition of the phases at a qualitative level is characterized by the shape and color gradation of the markers, and the arrows and their width indicate the direction of reactions of neighboring alloys and the proportion of phases. The number of components in the phase is related to the shape of the markers. The stability of alloys is determined by the expression [12]

$$\begin{gathered}\Delta G = \Delta H - TS;\\ \Delta S_{ss} = k_{\mathrm{B}}\sum_{i=1}^{n} x_i \ln x_i = R\ln(n),\end{gathered} \tag{1}$$

where G is the Gibbs free energy; ΔH is the enthalpy of mixing; ΔS_{ss} is the entropy of mixing of solid solutions; x_i is the mole fraction of the ith element in the HEA. Taking into account the separation into low-component reactants,

$$\Delta S_{ss} = R\ln\left(\frac{n}{n-1}\right).$$

Enthalpy ΔH of the n-atomic mixture is equal to

$$\Delta H = \sum_i \sum_{i>j} \Omega_{i,j} x_i x_j = \sum_i \sum_{i>j} \Omega_{i,j} \left(\frac{1}{n}\right)^2, \tag{2}$$

where $\Omega_{i,j}$ is a binary interaction and for the equiatomic composition is determined by the expression [18]

$$\Omega_{i,j} = 4\left[E_{ij}^{SQS} - \frac{1}{2}(E_i - E_j)\right], \tag{3}$$

where E_{ij}^{SQS} is the energy of the binary lattice, determined from first principles within the framework of the cluster approximation in ATAT [19]; E_i and E_j are the lattice energies of components. The results of stability calculations using formula (1) are shown in Fig. 1. The stability of the CrMnFeCoNi alloy was assessed in the temperature range $\Delta T = 300–1795$ K. The enthalpy of formation and mixing are generally negative. However, the enthalpy of mixing at temperatures below ~800 K is near the zero level, and, therefore, the 5-element CrMnFeCoNi alloy is prone to relaxation. The search for CrMnFeCoNi lattices with complete structural information can be implemented using the USPEX evolutionary method [13, 14]. In this article, the standards of the equiatomic fixed composition of CrMnFeCoNi and MnFeCoNi were studied in the USPEX code. The forecast was implemented under the following conditions: the proportion of generations generated from random structures and due to heredity was 0.3 and 0.5, respectively, while generation from mutations was 0.2. The fraction of the current generation that was used to generate the next generation was equal to 0.6. In each generation, populations of 30 atoms were considered and the initial number was also equal to 30 atoms. The calculations were performed with six optimization steps within the electron density functional in the electron density gradient pseudopotential (GGA) in the VASP code. The total lattice energy was determined at 0 K. Calculations of the orbitals of electronic states, the distribution of one-electron density, and the energy of the ground state were carried out in a self-consistent manner. The wave functions of valence electrons of atoms of phases of different generations were analyzed on the basis of plane waves with a kinetic energy cutoff radius of 330 eV. In this case, the total energy convergence was ~0.5×10^{-6} eV/atom. The equilibrium state and temperature dependences of the thermodynamic and mechanical properties were calculated in vaspkit [15] and phonopy [16] with the Vasp

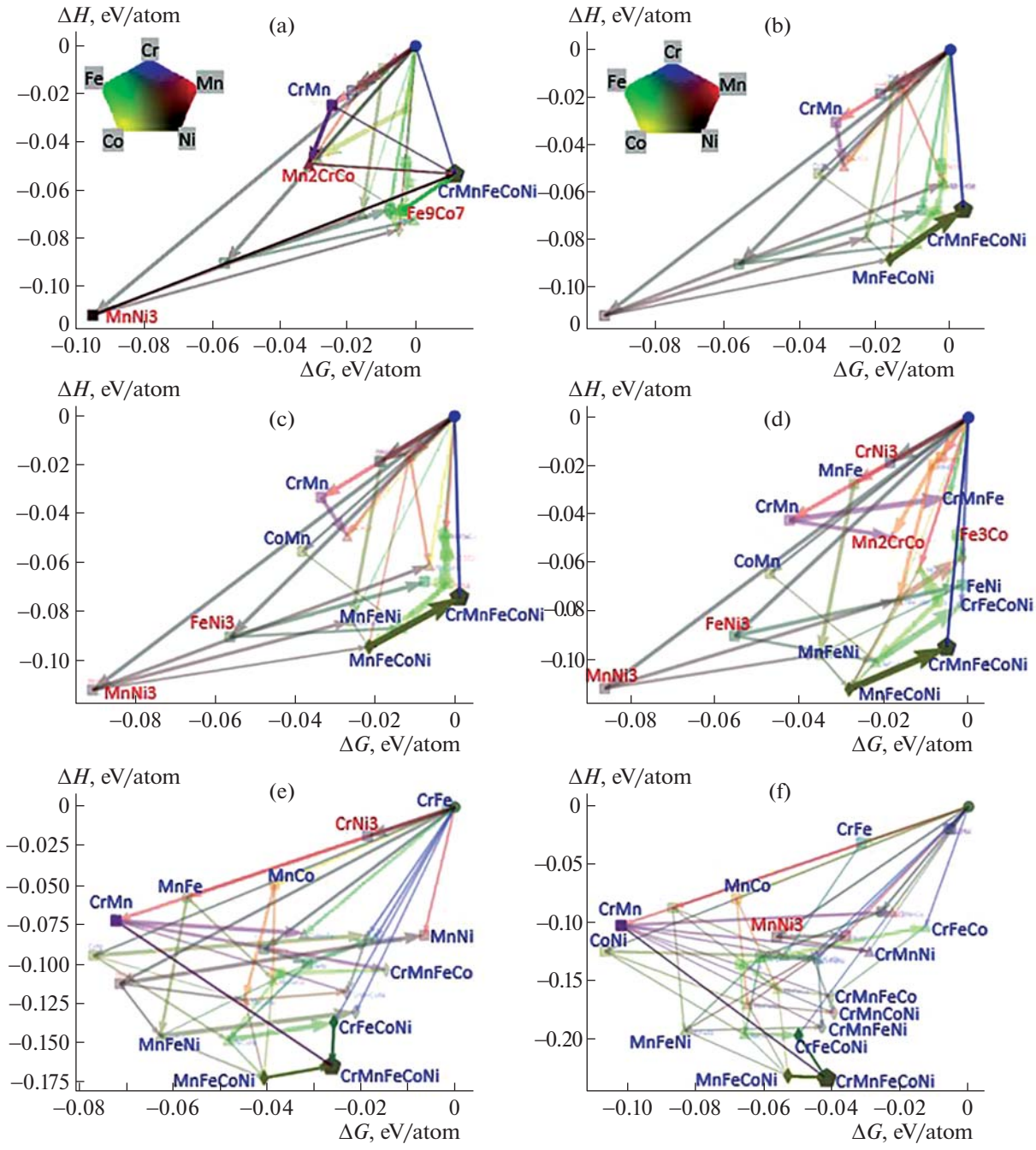

Fig. 1. Inverse convex hull of the HEA CrMnFeCoNi at different temperatures: T = (a) 700, (b) 800, (c) 850, (d) 1000, (e) 1500, and (f) 1795 K.

interface. The input data were the CrMnFeCoNi and MnFeCoNi lattices both in the initial state and after volumetric deformation.

RESULTS AND DISCUSSION

(1) According to the physical and mechanical characteristics of the CuCrMnFeCoNi coating, it should be noted that the level of its strength properties is at the level of hardened steel 40KhN2MA with a fairly high resistance to both elastic (1.5 times) and plastic deformation (2.5 times), which significantly affects the adhesive properties of the coating–substrate.

Table 1. Effective melting temperature of binary alloys

Binary alloys	T_{melt}, K	ΔH, kJ/mol	ΔS, kJ/mol
CrMn	1827.5	2.139	10.54
CrFe	1973.5	–1.444	11.37
CrCo	1952	–4.305	11.25
CrNi	1932	–6.387	11.13
MnFe	1665	0.286	9.59
MnCo	1643.5	–4.929	9.469
MnNi	1623.5	–7.739	9.354
FeCo	1789.5	–0.5491	10.31
FeNi	1769.5	–1.47	10.2
CoNi	1748	–0.206	10.7

Table 2. HEA structural parameters

Phase	A, Å	b, Å	c, Å	α, deg	β, deg	γ, deg	V, Å^3	F, eV	Space group
CrMnFeCoNi	4.1853	4.1853	4.1853	90	90	90	73.315	–6375.86	$P1$, Triclinic
MnFeCoNi	3.4759	3.4759	3.4759	90	90	90	41.997	–3915.67	

(2) The use of the magnetron method of applying the CuCrMnFeCoNi coating compared to other HEA coatings allowed the following: (1) increase in the rate of coating deposition; (2) obtaining coatings of great thickness (h = 10–15 μm); (3) providing tribological tests under specified conditions (V = 1 mm/s, N = 5 N) of high wear resistance and a low friction coefficient (μ = 0.07–0.1).

(3) For enthalpy estimates H_{mix} of the HEA CrMnFeCoNi, it is necessary to use the following binary alloys with a cubic lattice: AlNi, AlNb, AlTi, AlCo, NiNb, NiTi, NiCo, NbTi, NbCo, and TiCo. The melting point of binary alloys was estimated using the formula

$$T_{melt} = \sum c_i T_i,$$

where T_i is the melting temperature of the CrMnFeCoNi alloy elements. For metals Cr, Mn, Fe, Co, and Ni, the temperatures are equal to T_{melt} = 2136, 1519, 1811, 1768, and 1728 K, respectively. The effective melting temperatures of CrMnFeCoNi and MnFeCoNi found by formula (2) are equal to T_{melt} = 1792 and 1706 K, respectively. The melting temperatures of binary alloys are given in Table 1. Based on the obtained values for T_{melt} and known elements, the enthalpy of mixing was determined, as was the entropy contribution to the free energy of binary alloys within the framework of the Miedema model [20]. The calculation results are given in Table 1. It should be noted that not all of the binary alloys listed are stable. In particular, the unstable alloys include CrMn and MnFe. Using the InverseHubWeb method, the single-phase HEA CrMnFeCoNi was found to be stable below the melting point. It turns out to be interesting that the 4-element MnFeCoNi alloy is also stable, up to $T \approx$ 300 K. The HEA stability results for CrMnFeCoNi are presented in Fig. 1.

In this article, the search for 5-element lattices of CrMnFeCoNi, as well as MnFeCoNi, was implemented by the evolutionary method in USPEX [13, 14]. During the prediction process, about 300 and 420 standards of fixed compositions of CrMnFeCoNi and MnFeCoNi, respectively, were discovered, from which structures of the orthogonal class with space groups 47 and 25, respectively, were selected. After conversion to $P1$, estimates of the lattice energy in the CASTEP code, and details of the code are discussed in [21], the lattices of equiatomic composition for CrMnFeCoNi and MnFeCoNi with the lowest energy were identified, for which the equilibrium state was additionally determined in the vaspkit code [15]. The lattices presented in Table 1 correspond to stable and equilibrium states.

It should also be noted that for all SC lattices the atomic coordinates are known, however, due to the large volume, these data are not presented in this article. Table 2 shows the energies of equilibrium lattices calculated in the CASTEP code.

Table 3. Approximation parameters in the Vinet model

Phase	V_0, Å^3	F_0, eV	B_0, GPa	B_p'
CrMnFeCoNi	73.316	−31.575	129.583	2.249
MnFeCoNi	41.996	−29.128	254.813	2.745

This paper conducted a study of the energy of SC gratings as a function of volume variation based on the equation of state. The thermodynamic equation of state (EOS), which relates the internal energy, pressure, and lattice volume, plays an important role in predicting the structural and thermodynamic properties of materials at high temperatures, which allows, in particular, the search and determination of the equilibrium state of the lattice. At the initial stage, this article used the equation in the Vinet formulation [15]

$$F = F_0 + \frac{BV_0}{C^2}\left[1 - \left(1 + C\left(V^{1/2} - 1\right)\right)e^{C(V^{1/2}-1)}\right],$$

where $V = V/V_0$; V_0 and F_0 are the volume and energy at zero pressure, respectively. The volume modulus value B and its derivative with respect to pressure B_p were found after approximating (3) the dependence of energy on the lattice volume; the approximation parameters are given in Table 3.

Within the quasi-harmonic approximation (QHA), the Helmholtz free energy is written as

$$F(V,T) = E_0(V) + F_{\text{vib}}(V,T) + F_{\text{elec}}(V,T),$$

where E_0 is the lattice energy at 0 K; F_{vib} and F_{elec} are the phonon and electronic contributions to the free energy; V is the current lattice volume. The phonon contribution to the free energy is determined from the phonon density of states

$$F_{\text{vib}}(V,T) = k_{\text{B}}T\sum_{q,\lambda}\ln\left\{2\sin h\left(\frac{h\omega_{q,\lambda}(V)}{2k_{\text{B}}T}\right)\right\},$$

where k_{B}, h, and $\omega = 2\pi\nu$ are Boltzmann's constant, Planck's constant, and the frequency, respectively. The summation is carried out over all phonon branches and wave vectors of the 1st Brillouin zone. The electronic contribution F_{elec} at low temperatures, as a rule, is insignificant, so its correction was not made. The specific heat capacity of the phonon was determined by the formula

$$C_{\text{v}}^{\text{vib}} = \sum_{q,\lambda} k_{\text{B}}\cosh^2\left(\frac{h\omega_{q,\lambda}(V)}{2k_{\text{B}}T}\right)^2.$$

If the temperature dependence of the lattice expansion $\alpha(T)$ is known, or the Grüneisen parameter, then based on the EOS equation, it is possible to calculate various thermodynamic characteristics. The Phonopy code uses the EOS equation in the Birch–Murnaghan formulation [16]

$$F(V) = F_{\text{eq}} + \frac{BV_0}{B_p}\left[\frac{(V_{\text{eq}}/V)^{B_p}}{B_p - 1} - 1\right] - \frac{BV_0}{B_p - 1},$$

where F_0, B, V_0, and B_p are approximating parameters. The Grüneisen parameter γ is equal to the volume derivative of the dynamic matrix, which also depends on the wave vectors of the known phonon branches in the first Brillouin zone. The temperature dependence $\gamma(T)$ allows us to predict the parameter $\alpha(T)$, as well as the specific heat capacity C_v. The results of calculations of the thermodynamic and mechanical characteristics of the HEAs CrMnFeCoNi and MnFeCoNi are shown in Figs. 2 and 3.

The thermodynamic properties of the HEAs CrMnFeCoNi and MnFeCoNi (Figs. 2d, 3d) were calculated in the Debye model, and the remaining properties were calculated within the QHA approximation (the thermal expansion of the lattice was taken into account). The results were not normalized to the number of atoms. From the results obtained, it follows that, with increasing temperature, the lattice energy in the equilibrium state in the HEAs CrMnFeCoNi and MnFeCoNi decreases significantly. The lattice volume, the coefficient of thermal expansion, the bulk modulus of elasticity, and the Grüneisen parameter, in which a slight deviation from the linear dependence is observed, increase noticeably. The specific heat capacity increases significantly in the temperature range under study, with the most intense growth found in the range up to ~300 K. In the MnFeCoNi alloy, the intensity of growth turns out to be significantly

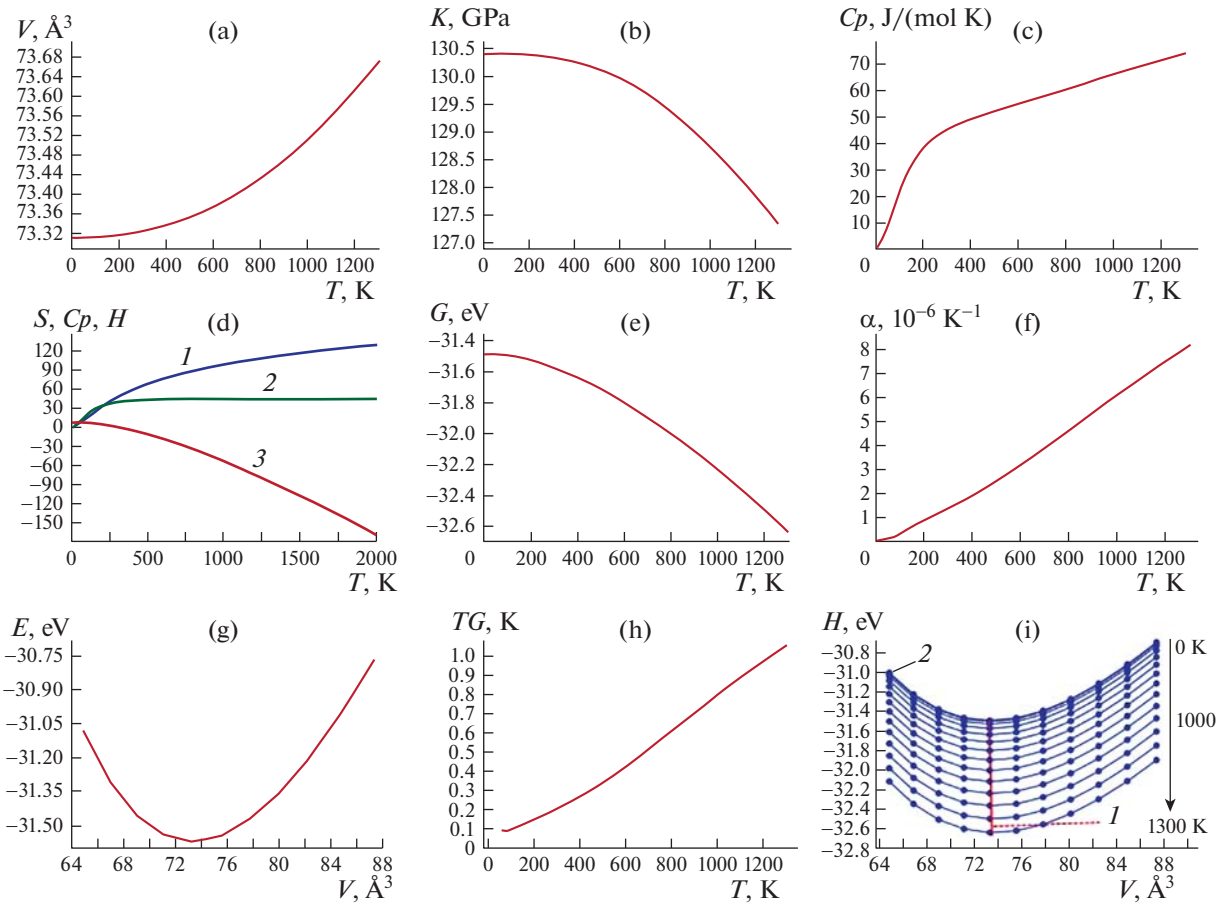

Fig. 2. Thermomechanical properties of the HEA CrMnFeCoNi depending on temperature: (a) lattice volume; (b) bulk modulus of elasticity; (c) specific heat; (d) thermodynamic properties: *1*, entropy *S*, J/K/mol; *2*, phonon specific heat capacity C_v, J/K/mol; *3*, enthalpy *H*, kJ/mol; (e) Gibbs energy; (f) coefficient of thermal expansion; (g) energy of a unit cell depending on volume; (h) Grüneisen coefficient; (i) free lattice energy versus volume at different temperatures: equilibrium free energy *1* and the dependence of free energy on volume at different temperatures *2*.

lower than in HEA CrMnFeCoNi at high temperatures. The Gibbs free energy decreases significantly with increasing temperature. The temperature dependences of the entropy and bulk elastic moduli are of interest. In a 5-element HEA, the entropy is approximately half that of a 4-element alloy. In the 4-element HEA MnFeCoNi, the bulk module significantly exceeds (*B* approximately two times) the value for the HEA CrMnFeCoNi at all temperatures studied. The normalized free energies of the HEAs CrMnFeCoNi and MnFeCoNi lattices in the temperature range $T \approx 0$–800 K vary within $F \approx$ –6.3...–6.5, –7.4...–7.63 eV/atom, respectively. Ab initio calculations of the free energies indicate that the equilibrium HEAs CrMnFeCoNi and MnFeCoNi belong to quasi-stable and stable alloys; however, CrMnFeCoNi is prone to relaxation in the direction of the average entropy composition, and MnFeCoNi, due to higher values of the bulk modulus of elasticity, is preferable in practice. A detailed analysis of the mechanical properties in the vaspkit code showed that MnFeCoNi with a face-centered lattice is a high-strength material. The spatial distribution of atoms in the lattice of the MnFeCoNi and CrMnFeCoNi alloys is shown in Fig. 4.

From calculations of the elastic constants from first principles presented in Table 4, it follows that the bulk modulus of elasticity, Young's modulus, and the shear modulus for both single crystals and polycrystals are characterized by high values.

The HEA MnFeCoNi is mechanically stable and prone to brittle fracture. The mechanical properties of the HEA MnFeCoNi are presented in Table 5.

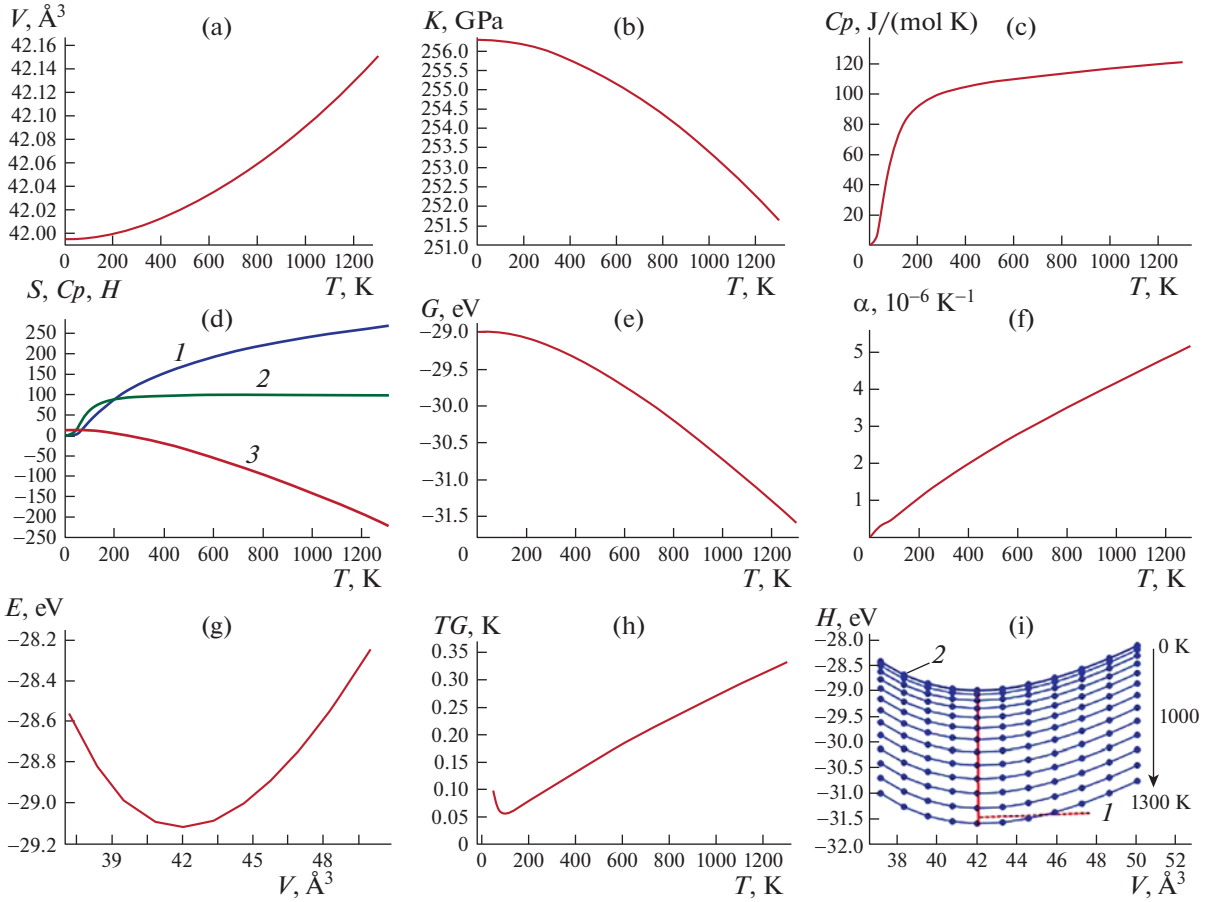

Fig. 3. Thermomechanical properties of the HEA MnFeCoNi depending on temperature: (a) lattice volume; (b) bulk modulus of elasticity; (c) specific heat; (d) thermodynamic properties: *1*, entropy S, J/K/mol; *2*, phonon specific heat capacity C_v, J/K/mol; *3*, enthalpy H, kJ/mol; (e) Gibbs energy; (f) coefficient of thermal expansion; (g) energy of a unit cell depending on the volume at 0 K; (h) Grüneisen coefficient; (i) equilibrium free energy *1* and the dependence of free energy on volume at different temperatures *2*.

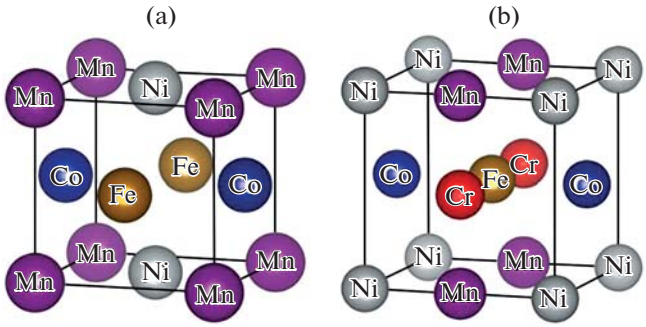

Fig. 4. Spatial distribution of atoms in the lattice: (a) MnFeCoNi; (b) CrMnFeCoNi.

The following conditions of mechanical stability are met for the alloy:

$$C_{11}, C_{44}, C_{55}, C_{66} \quad \text{have a positive sign;}$$

$$C_{11}C_{22} > C_{12}^2;$$

$$C_{11}C_{22}C_{33} + 2C_{12}C_{13}C_{23} - C_{11}C_{23}^{2^2} - C_{22}C_{13}^2 - C_{33}C_{12}^2 > 0.$$

Table 4. Tensor of elastic constants C_{ij} of the HEA MnFeCoNi (GPa)

394.192	210.412	198.504	0.000	0.000	0.000
210.412	390.368	171.549	0.000	0.000	0.000
198.504	171.549	389.176	0.000	0.000	0.000
0.000	0.000	0.000	153.476	0.000	0.000
0.000	0.000	0.000	0.000	200.852	0.000
0.000	0.000	0.000	0.000	0.000	218.400

Table 5. Mechanical properties of the HEA MnFeCoNi (GPa)

Parameter	Monocrystals			Polycrystals		
	minimum	maximum	anisotropy	Voigt	Reuss	Hill
Volume modulus (GPa)	236.117	300.622	1.273	259.41	258.791	259.099
Young's modulus (GPa)	245.093	457.864	1.868	385.88	348.772	367.494
Shear modulus (GPa)	90.432	218.392	2.415	154.10	136.732	145.415
Poisson's ratio	–0.011	0.503	–45.404	0.25	0.275	0.264

This article assessed the microhardness within the framework of the Oganov model [22]. The Vickers microhardness was found to be 17.56 GPa.

CONCLUSIONS

Thus, using the methods used in InverseHubWeb, USPEX, vaspkit, and phonopy, it was established that the HEA CrMnFeCoNi belongs to stable and equilibrium structures. The InverseHubWeb method also discovered a medium-entropy, single-phase HEA, MnFeCoNi, the stability range of which is $\Delta T \approx (300 - T_{\text{melt}})$ K. The stability range for CrMnFeCoNi is $\Delta T \approx (800 - T_{\text{melt}})$ K. Based on the crystallographic data from the HEA CrMnFeCoNi and MnFeCoNi in the USPEX code we selected fcc, and bcc equilibrium lattices with $P1$ symmetry. Within the framework of the QHA model, it was established that the medium-entropy equilibrium HEA MnFeCoNi has lower specific energy at finite temperatures compared to CrMnFeCoNi; it is mechanically stable, and it has higher strength properties, which are almost 1.5–2.0 times higher than the corresponding values for CrMnFeCoNi. The addition of Cu to the composition of CrMnFeCoNi powder targets significantly enhances the tribological characteristics of the resulting coatings, reducing the coefficient of friction and increasing wear resistance.

AUTHOR CONTRIBUTION

The study and analysis of the physical, mechanical, and tribological characteristics of experimental high-entropy vacuum ion-plasma coatings was carried out by V.I. Kolesnikov, I.V. Kolesnikov, and K.N. Polityko. The stability of high-entropy coatings was studied by Yu.A. Abzaev. The structures were predicted and validated by A.A. Guda, V.I. Kolesnikov, and S.A. Guda.

FUNDING

This work was supported by the Russian Science Foundation (project no. 21-79-30007).

CONFLICT OF INTEREST

The authors of this work declare that they have no conflicts of interest.

REFERENCES

1. Cantor, B., Chang, I.T.H., Knight, P., and Vincent, A.J.B., Microstructural development in equiatomic multicomponent alloys, *Mater. Sci. Eng., A*, 2023, vols. 375–377, pp. 213–218. https://doi.org/10.1016/j.msea.2003.10.257
2. Gludovatz, B., Hohenwarter, A., Catoor, D., Chang, E.H., George, E.P., and Ritchie, R.O., A fracture-resistant high-entropy alloy for cryogenic applications, *Science*, 2014, vol. 345, no. 6201, pp. 1153–1158. https://doi.org/10.1126/science.1254581
3. Otto, F., Dlouhý, A., Pradeep, K.G., Kubenov, M., Raabe, D., Eggeler, G., and George, E.P., Decomposition of the single-phase high-entropy alloy CrMnFeCoNi after prolonged anneals at inter-mediate temperatures, *Acta Mater.*, 2016, vol. 112, pp. 40–52. https://doi.org/10.1016/j.actamat.2016.04.0051359-64542016
4. Laplanche, G., Gadaud, P., Horst, O., Otto, F., Eggeler, G., and George, E.P., Temperature dependencies of the elastic moduli and thermal expansion coefficient of an equiatomic, single-phase CoCrFeMnNi high-entropy alloy, *J. Alloys Compd.*, 2014, vol. 623, pp. 348–353. https://doi.org/10.1016/j.jallcom.2014.11.061
5. Sahlberg, M., Karlsson, D., Zlotea, C., and Jansson, U., Superior hydrogen storage in high entropy alloys, *Sci. Rep.*, 2016, vol. 6, no. 1, p. 36770. https://doi.org/10.1038/srep36770
6. Senkov, O.N., Wilks, G.B., Scott, J.M., and Miracle, D.B., Mechanical properties of $Nb_{25}Mo_{25}Ta_{25}W_{25}$ and $V_{20}Nb_{20}Mo_{20}Ta_{20}W_{20}$ refractory high entropy alloys, *Intermetallics*, 2011, vol. 19, no. 5, pp. 698–706. https://doi.org/10.1016/j.intermet.2011.01.004
7. Li, Zh., Pradeep, K.G., Deng, Yu., Raabe, D., and Tasan, C.C., Metastable high-entropy dual-phase alloys overcome the strength–ductility trade-off, *Nature*, 2016, vol. 534, no. 7606, pp. 227–230. https://doi.org/10.1038/nature17981
8. Li, R., Xie, L., Wang, W.Yi., Liaw, P.K., and Zhang, Yo., High-throughput calculations for high-entropy alloys: A brief review, *Front. Mater.*, 2020, vol. 7, p. 290. https://doi.org/10.3389/fmats.2020.00290
9. Lee, K., Ayyasamy, M.V., Delsa, P., Hartnett, T.Q., and Balachandran, P.V., Phase classification of multi-principal element alloys via interpretable machine learning, *npj Comput. Mater.*, 2022, vol. 8, no. 1, p. 12. https://doi.org/10.1038/s41524-022-00704-y
10. Abzaev, Yu.A., Guda, S.A., Guda, A.A., Zelenkov, A.A., and Kolesnikov, V.I., Structural phase state of high-entropy NbTiHfVZr alloy, *Phys. Met. Metallogr.*, 2023, vol. 124, no. 8, pp. 807–815. https://doi.org/10.1134/s0031918x2360118x
11. Ivanov, Yu.F., Abzaev, Y.A., Gromov, V.E., Konovalov, S.V., Klopotov, A.A., and Semin, A.P., Phase analysis and structural state of AlCoFeCrNi high-entropy alloy of non-equiatomic composition, *AIP Conf. Proc.*, 2022, vol. 2509, p. 020087. https://doi.org/10.1063/5.0085244
12. Evans, D., Chen, J., Bokas, G., Chen, W., Hautier, G., and Sun, W., Visualizing temperature-dependent phase stability in high entropy alloys, *npj Comput. Mater.*, 2021, vol. 7, p. 151. https://doi.org/10.1038/s41524-021-00626-1
13. Oganov, A.R. and Glass, C.W., Crystal structure prediction using ab initio evolutionary techniques: Principles and applications, *J. Chem. Phys.*, 2006, vol. 124, no. 24, p. 244704. https://doi.org/10.1063/1.2210932
14. Oganov, A.R., Lyakhov, A.O., and Valle, M., How evolutionary crystal structure prediction works—and why, *Acc. Chem. Res.*, 2011, vol. 44, no. 3, pp. 227–237. https://doi.org/10.1021/ar1001318
15. Wang, V., Xu, N., Liu, J.-C., Tang, G., and Geng, W.-T., VASPKIT: A user-friendly interface facilitating high-throughput computing and analysis using VASP code, *Comput. Phys. Commun.*, 2021, vol. 267, p. 108033. https://doi.org/10.1016/j.cpc.2021.108033
16. Togo, A., Oba, F., and Tanaka, I., First-principles calculations of the ferroelastic transition between rutile type and $CaCl_2$-type SiO_2 at high pressures, *Phys. Rev. B*, 2008, vol. 78, no. 3, p. 134106. https://doi.org/10.1103/PhysRevB.78.134106

17. Golovin, Yu.I., *Nanoindentirovanie i ego vozmozhnosti* (Nanoindentation and Its Possibilities), Moscow: Mashinostroenie, 2009.
18. *GOST* (State Standard) *8.748-2011 (ISO 14577-1:2002): State system for ensuring the uniformity of measurements. Metallic materials. Instrumented indentation test for hardness and materials parameters. Part 1. Test method*, 2013.
19. Bäker, M., Calculating phase diagrams with ATAT, *arXiv Preprint*, 2019. https://doi.org/10.48550/arXiv.1907.10151
20. Zhang, R.F., Zhang, S.H., He, Z.J., Jing, J., and Sheng, S.H., Miedema Calculator: A thermodynamic platform for predicting formation enthalpies of alloys within framework of Miedema's theory, *Comput. Phys. Commun.*, 2016, vol. 209, pp. 58–69. https://doi.org/10.1016/j.cpc.2016.08.013
21. Kosmachev, P.V., Abzaev, Yu.A., and Vlasov, V.A., Quantitative phase analysis of plasma-treated high-silica materials, *Russ. Phys. J.*, 2018, vol. 61, no. 2, pp. 264–269. https://doi.org/10.1007/s11182-018-1396-4
22. Mazhnik, E. and Oganov, A.R., Application of machine learning methods for predicting new superhard materials, *J. Appl. Phys.*, 2020, vol. 128, no. 7, p. 75102. https://doi.org/10.1063/5.0012055